Published in final edited form as:
Chromosoma. 2008 October ; 117(5): 471–485. doi:10.1007/s00412-008-0167-3.

REGULATION OF THE MEIOTIC PROPHASE I TO METAPHASE I TRANSITION IN MOUSE SPERMATOCYTES

Fengyun Sun and **Mary Ann Handel**
The Jackson Laboratory 600 Main Street Bar Harbor, ME 04609 USA

Abstract

The meiotic prophase I to metaphase I transition (G2/MI) involves disassembly of synaptonemal complex (SC), chromatin condensation, and final compaction of morphologically distinct MI bivalent chromosomes. Control of these processes is poorly understood. The G2/MI transition was experimentally induced in mouse pachytene spermatocytes by okadaic acid (OA), and kinetic analysis revealed that disassembly of the central element of the SC occurred very rapidly after OA treatment, before histone H3 phosphorylation on Ser10. These events were followed by relocalization of SYCP3 and final condensation of bivalents. Enzymatic control of these G2/MI transition events was studied using small molecule inhibitors: butyrolactone I (BLI), an inhibitor of cyclin-dependent kinases (CDKs) and ZM447439 (ZM), an inhibitor of aurora kinases (AURKs). The formation of highly condensed MI bivalents and disassembly of the SC are regulated by both CDKs and AURKs. AURKs also mediate phosphorylation of histone H3 in meiosis. However, neither BLI nor ZM inhibited disassembly of the central element of the SC. Thus, despite evidence that MPF is a universal regulator of the onset of cell division, desynapsis, the first and key step of the G2/MI transition, occurs independently of BLI -sensitive CDKs and ZM-sensitive AURKs.

Introduction

When meiotic germ cells leave the lengthy prophase I of meiosis by passing through the diplotene stage to the first meiotic metaphase (a process known asthe G2/MI transition), a number of events occur. Morphologically, the most dramatic of these is the remodeling of chromatin from the relatively dispersed state of prophase to form highly condensed, metaphase chromosomes. This is accompanied by disassembly and/or reorganization of components of the synaptonemal complex (SC). While it is presumed that these events do not occur until after completion of meiotic recombination, the precise relationship between the culmination of recombination and the onset of the G2/MI transition is not known; nor have the proximal regulators and signaling pathways that govern this process been resolved. Here we focus on the disassembly of the SC as a signature event of the G2/MI transition, and determine different mechanisms for removal and relocalization of different SC components, in the context of the concurrent events of histone H3 phosphorylation on Ser10 and condensation and formation of morphologically distinct bivalents.

The SC is a meiosis-specific, zipper-like tripartite protein complex that lies between synapsed homologous chromosomes, and may mediate synapsis and/or recombination (Crane et al. 2004; Dobson et al. 1994; Hunter 2003; Von Wettstein 1984; Zickler and Kleckner 1999). The lateral elements (LEs) of the SC are thought to coincide with the axes of each of the two paired, but non-sister, homologs. Components of the LEs include two SC proteins, SYCP2 (Offenberg et al. 1998)and SYCP3 (Dobson et al. 1994; Heyting et al. 1985; Heyting et al. 1987), both of

Direct correspondence to: Mary Ann Handel Email: maryann.handel@jax.org, Tel: 207-288-6778, Fax: 207-288-6073.

which have been shown by genetic analysis to be essential for formation of the chromosomal axes and mature SC (Kouznetsova et al. 2005; Yang et al. 2006; Yuan et al. 2000). Other proteins essential for the formation of the SC LEs are cohesins (Eijpe et al. 2000). Cohesins belong to the structural maintenance of chromosomes (SMC) family, and include meiosis-specific cohesin subunits REC8 (Eijpe et al. 2003), STAG3 (Pezzi et al. 2000) and SMC1B (Revenkova et al. 2001). Genetic analyses have revealed that SMC1B and REC8 are important for the integrity of the LEs and SC (Bannister et al. 2004; Revenkova et al. 2004; Xu et al. 2005). The central element of the SC bridges the two LEs through an array of transverse filaments, and is comprised in part by the protein SYCP1 (Dobson et al. 1994; Meuwissen et al. 1992); synapsis does not occur in mice lacking this protein (De Vries et al. 2005). Other proteins interacting within the central element include SYCE1 and SYCE2 (Costa et al. 2005)and TEX12 (Hamer et al. 2006). SYCE2 has been shown to be required for assembly of the SC (Bolcun-Filas et al. 2007).

The SC disassembles as meiotic cells progress from the pachytene stage, when recombination occurs, through diplonema and into the meiotic division phase. The hallmark of exit from the pachytene stage to the diplotene stage is desynapsis. Desynapsis enables homolog separation and is marked cytologically by the removal of the central element of the SC, when immunolabeling of SYCP1 is lost from the SC (Moens 1995). Subsequently, SYCP3 labeling redistributes within and from the LEs of the SC and is found in the centromeric regions (Dobson et al. 1994), and also in patches between sister chromatids (Parra et al. 2004; Prieto et al. 2001; Viera et al. 2003). Experimental induction of the G2/MI transition with the phosphatase inhibitor OA recapitulates desynapsis, homolog separation and redistribution of SYCP3 from the LEs in mouse spermatocytes (Cobb et al. 1999a; Handel et al. 1995; Tarsounas et al. 1999; Wiltshire et al. 1995). These events of disassembly of the SC occur coordinately with other key aspects of chromatin remodeling events in the G2/MI transition, including phosphorylation of histone H3 on Ser10, a marker of entry into M-phase (Hendzel et al. 1997), and the final compaction and formation of morphologically distinct bivalents (MI chromosomes). Mechanisms of chromatin condensation and formation of compact bivalents are not well understood in either mitosis or meiosis (Belmont 2006). Although controversial, it is likely that both DNA topoisomerase IIα and condensins are involved in the various stages in the formation of fully condensed chromosomes, and, in all probability, the process is driven by the same kinases that regulate mitotic cell cycle progress (Belmont 2006; Swedlow and Hirano 2003). But whether these diverse events of the meiotic G2/MI transition are under common control is not known.

The “universal” regulator of metaphase onset, MPF (metaphase promoting factor) probably plays a predominant role in chromatin remodeling during the G2/MI transition of mouse spermatocytes. MPF, comprised of a catalytic subunit, CDC2A (formerly known as CDK1), and a regulatory cyclin subunit, cyclin B1 (CCNB1), is regulated by phosphorylation and de-phosphorylation by cell cycle-related kinases and phosphatases. The CDC2A kinase is present in pachytene spermatocytes (Cobb et al. 1999a; Godet et al. 2000). The finding that the phosphatase inhibitor OA prompted the meiotic G2/MI transition in mouse spermatocytes (Handel et al. 1995; Wiltshire et al. 1995)suggested that MPF, or other kinases, could be involved. Roscovitine inhibition of cyclin-dependent kinases impedes formation of post-meiotic germ cells in co-cultures of rat germ cells and Sertoli cells (Godet et al. 2004), and both a broad-spectrum cyclin-dependent kinase inhibitor (staurosporine) and a more specific CDK inhibitor butyrolactone I (BLI) inhibit the formation of condensed bivalents induced by OA treatment of mouse spermatocytes (Cobb et al. 1999a). However, which steps of SC disassembly and other dynamics of chromatin remodeling MPF and/or other G2 cyclin-dependent kinases regulate during the G2/MI transition is not established.

Kinases other than MPF must also be involved in the spermatocyte's G2/MI transition. The most compelling evidence for this is that inhibition of MPF does not inhibit phosphorylation of histone H3 on Ser10, a characteristic marker of the meiotic G2/MI transition (Cobb et al. 1999a). The MAP kinases MAPK3/1 have been implicated in the process (Sette et al. 1999), but genetic evidence argues that this may not be the case (Colledge et al. 1994; Hashimoto et al. 1994; Inselman and Handel 2004). Other candidate kinases for the G2/MI transition include the serine-threonine aurora kinases (AURKs), which have been demonstrated to play roles in the mitotic G2/M transition (Carmena and Earnshaw 2003)and phosphorylation of histone H3 on Ser10 (Arlot-Bonnemains et al. 2001; Crosio et al. 2002). Inhibitors that specifically target AURKs, such as ZM447439 (ZM), have helped establish the evidence that they phosphorylate histone H3 on Ser10 in mitosis (Ditchfield et al. 2003; Gadea and Ruderman 2005). AURKs are expressed in oocytes (Jelinkova and Kubelka 2006; Yao and Sun 2005; Yao et al. 2004), in G2 phase mouse spermatocytes (Chieffi et al. 2004; Kimmins et al. 2007; Parra et al. 2003 ; Tang et al. 2006), and localize in spermatocyte chromatin (Hashimoto et al. 1994; Kimmins et al. 2007)and centromeres at the late diplotene stage (Parra et al. 2003); thus they are in the right place at the right time to function in the G2/MI transition. Expression of a kinase-inactive mutant AURKB resulted in abnormal germ cell – somatic cell relationships and an increase in apoptotic spermatocytes at metaphase in AURKB mutant mice (Kimmins et al. 2007), but functional roles for AURKs specifically in the spermatocyte's G2/MI transition have not yet been experimentally demonstrated.

Here, OA-induced G2/MI transition was used as an experimental model to determine if disassembly of SC structure, phosphorylation of histone H3 on Ser10 and condensation and compaction of bivalents are under common cell cycle control or differentially regulated in mouse spermatocytes. We show that disassembly of the central element of the SC (removal of SYCP1 from the SC) occurred rapidly after OA treatment, before phosphorylation of histone H3 on Ser10. This was followed by relocalization of SYCP3 in the SC LEs and then by condensation and formation of morphologically distinct bivalents. ZM inhibition demonstrated a role for AURKs in both histone H3 phosphorylation on Ser10 and SC remodeling during the meiotic G2/MI transition. Disassembly of the central element and LEs of the SC after OA treatment were differentially regulated: BLI-sensitive CDKs and ZM-sensitive AURKs directly or indirectly control removal and relocalization of SYCP3 in the LEs, but their inhibition did not affect initiation of desynapsis and disassembly of the SC central element.

Materials and Methods

Animals

Male (C57BL/6J X SJLT) F1 mice (herein designated as B6SJL), aged 8 weeks were used in this study. All mice were bred and raised in the research colony of the authors at The Jackson Laboratory. The protocols for their care and use were approved by the Institutional Animal Care and Use Committee (IACUC) of The Jackson Laboratory.

Spermatocyte collection and culture conditions

Adult B6SJL males were used as the source of testes for preparation of highly enriched fractions of pachytene spermatocytes. The isolation of pachytene spermatocytes was performed as previously described (Bellve 1993). In brief, detunicated testes were placed into Krebs-Ringer bicarbonate solution (KRB: 120.1 mM NaCl, 4.8 mM KCl, 25.2 mM $NaHCO_3$, 1.2 mM KH_2PO_4, 1.2 mM $MgSO_4.7H_2O$, 1.3 mM $CaCl_2$, 11 mM glucose, 1 X essential amino acids, 1 X nonessential amino acids), and digested with 0.5 mg/ml collagenase (Sigma) and then with 0.5 mg/ml trypsin (Sigma). The released cells were washed with KRB containing 0.5% bovine serum albumin (BSA) (Sigma), and then sedimented at unit gravity through a 2 – 4% BSA gradient generated in a medium-size STA-PUT chamber (Johns Scientific, Ontario). After 2.5

hours, 300-drop fractions were collected at a rate of 1/43 sec. Cells in these fractions were assessed for morphology and purity by light microscopy using Normarski optics. The average purity of the pachytene spermatocyte fractions used was greater than 80%. The pooled pachytene spermatocyte fractions were washed once and then resuspended in HEPES (25 mM)-buffered MEMα culture medium (Sigma) supplemented with 25 mM $NaHCO_3$, 5% fetal bovine serum (Atlanta Biologicals), 10 mM sodium lactate, 59 μg/ml penicillin, 100 μg/ml streptomycin (Handel et al. 1995). Spermatocytes (2.5 x 10^6cells/ml) w ere subjected to short-term culture at 32°C in 5% CO_2as previously described (Handel et al. 1995).

After overnight culture, the pachytene spermatocytes were induced to undergo the G2/MI transition by the addition of OA (CalBiochem), dissolved at 244 μM in ethanol and used at 5 μM in the culture, while control cells were treated with the same volume of ethanol (Handel et al. 1995; Wiltshire et al. 1995). To inhibit CDKs, spermatocytes were incubated with 100 μM butyrolactone I (BLI, CalBiochem) (Cobb et al. 1999b). To inhibit AURKs, spermatocytes were treated with ZM 447439 (ZM, AstraZeneca) (Ditchfield et al. 2003). ZM was used at 5 μM, based both on the manufacturer's recommendation and our experiments. These inhibitors were added 0.5 hour prior to the OA addition, and the controls were treated with vehicle alone. For kinetic analyses, spermatocytes were harvested and processed for microscopy analysis at 0, 0.5, 1.0, 1.5, 2.0, 3.0, 4.0, and 5.0 hours after the treatment. Cells were scored for presence, absence and pattern of labeling with antibodies recognizing SYCP1, SYCP3, and histone H3 phosphorylated on Ser10. Differences from control (untreated) spermatocytes were tested for significance by a paired t-test.

Cytological analyses

For immunofluorescence analysis, cells were collected by centrifugation, surface-spread in wells of multispot microscope slides (Shandon, Pittsburgh, PA) and fixed following the procedure previously described (Cobb et al. 1999a; Cobb et al. 1997). Prior to antibody labeling, slides were washed three times in washing/blocking buffer (0.3% BSA, 1% goat serum in phosphate-buffered saline, pH 7.4); the second wash included 0.05% Triton-X 100. After draining, the slides were incubated with primary antibodies. Antibodies and dilution used were: rabbit anti-SYCP1 (a gift from C. Heyting) used at 1:1000 dilution or rabbit anti-SYCP1 (Novus, NB 300-229) used at 1:100 dilution; polyclonal rat anti-SYCP3 (Eaker et al. 2001) used at 1:1000 dilution or mouse anti-SYCP3 (Novus, NB100-2065) used at 1:100 dilution; rabbit anti-phosphorylated histone H3 on Ser10 (Abcam, ab14955) used at 1:1000 dilution; rabbit anti-STAG3 (Santa Cruz, sc-20345) used at 1:200 dilution, and rabbit anti-REC8 (a gift from C. Heyting) used at 1:250 dilution. Secondary antibodies against rabbit, rat or mouse IgG and conjugated with Alexa 594 or 488 (Molecular Probes) were used at 1:500 dilution. Images were acquired with a Leica DMRXE epifluorescence microscope equipped with a 100X planneofluar oil-immersion objective lens and a triple filter (set no. 61000V2 BS&M, Chroma Technology, Rockingham, VT) for simultaneous visualization of green (Alexa 488), red (Alexa 594), yellow (Alexa 488 + Alexa 594) and blue (DAPI) fluorescence. The microscope is linked to a Micromax cooled CCD camera (RS Princeton Instrument), a high-speed shutter driven by a Sutter Lambda 10-2 (Sutter Instrument)and Metamorph software (Universal Imaging Corporation)to capture the images.

Chromosome condensation was evaluated from air-dried chromosome preparations (Evans et al. 1964) from cultured spermatocytes collected by centrifugation and washed in 2.2% sodium citrate. The air-dried chromosome preparations were stained with Gurr Giemsa (Invitrogen). G2/MI stages, from pachynema to MI were scored using an Olympus microscope with a 40X plan objective and 10X ocular lenses, and images were captured to Adobe Photoshop with a Hamamatsu C5810 color-chilled camera (Photonic System, Bridgewater, NJ).

Western blotting

Equal numbers of cells from control and OA-treated cultures were washed twice with cold phosphate-buffered saline (PBS); cell pellets were suspended, at 10^8cell/ml, and lysed in RIPA buffer (Santa Cruz) containing protease inhibitor cocktail (Santa Cruz). After centrifugation, the supernatant was mixed with an equal volume of 2X sample buffer (Santa Cruz), and boiled for 5 min. A lysate containing 15 μg protein from each sample group was loaded and electrophoresed on an 8% SDS-polyacrylamide gel and transferred to PVDF membrane (Millipore) using a semi-dry transfer apparatus (Bio-Rad) with Tris-glycine buffer, pH 8.3. After transfer, the membrane was blocked in blocking buffer (LI-COR) at 4°C overnight. The blots were probed with anti-SYCP1 or anti-SYCP3 (each at a 1:2000 dilution) at room temperature for 1 h with gentle shaking. After 4 x 5 minute washes with PBS containing 0.1% Tween-20, blots were incubated with Irdye800-conjugated secondary antibody (Rockland), 1:5000 dilution, for 45 min at room temperature. After three washes with PBS containing 0.1% Tween-20 and one rinse with PBS, the blots were scanned with an Odyssey infrared imaging system (LI-COR).

In-gel kinase assay

The in-gel kinase assay was conducted according to previously reported methods (Wooten 2002). Briefly, spermatocytes from different conditions of OA and ZM were lysed at a concentration of 10^8cells per ml directly in lysis buffer (20 mM Tris -HCl, pH 7.5, 137 mM NaCl, 1 mM $MgCl_2$, 1 mM Na_3OV_4, 100 μM NaF, 1.0% NP-40, 10 mM β-glycerophosphate, 10% glycerol, 1 mM phenylmethanesulfonyl fluoride, 10 μg/ml leupeptin, 5 μg/ml aprotinin, 2.5 μg/ml p-Nitrophenylphosphate, PnPP). The lysate was then centrifuged at 12,000 x g for 10 minutes at 4°C and the supernatant was transferred to another tube. An equal amount of loading buffer (0.5 M Tris-HCl, pH 6.8, 4% SDS, 10% β-mercaptoethanol, and 20% glycerol) was added to each supernatant, and the samples were boiled for 5 minutes. A volume equivalent to 15 μg protein was loaded on gels containing 0.25 mg of calf thymus histone H3 (Boehringer) per ml or 0.25 mg of bovine serum albumin per ml in the separating portions. After electrophoresis, SDS was removed by washing the gel first with a solution of 20% 2-propanol and 50 mM Tris-HCl (pH 8.0), and then with 50 mM Tris-HCl (pH 8.0) and 1mM dithiothreitol (DTT). Proteins were denatured by treating the gel with buffer (50 mM Tris-HCl (pH 8.0), 20 mM DDT, 6 M guanidine hydrochloride), and then treated overnight at 4°C with renaturing solution (50 mM Tris-HCl (pH 8.0), 5 mM DDT, 0.04% Tween-20, 100 mM NaCl, 5 mM $MgCl_2$). After one wash in the assay buffer (25 mM Hepes, pH 7.4, 20 mM $MgCl_2$1 mM $MnCl_2$, 5 mM NaF, 100 μM Na_3OV_4, 2.5 μg/ml PnPP and 1 mM DTT), the gels were incubated for 2.0 h at room temperature in assay buffer containing 50 μM ATP and 20 μCi/ml [γ^{32}P]-ATP (PerkinElmer). After four extensive washes with 5% trichloroacetic acid, 1% sodium pyrophosphate, the gels were dried onto two sheets of filter paper and covered with plastic wrap. FUJIFILM FLA5100 (Life Science, Japan) was used to image the gels and Multi Gauge (Life Science, Japan) was used for quantitative analysis.

Results

Disassembly of the SC central element initiates before the phosphorylation of histone H3 during the G2/MI transition

Because of the advantage of a large population of cells responding to a stimulus (OA), temporal order of events can be determined more precisely in vitro than by assessing spermatocytes within seminiferous tubules. The dynamics of SC and chromosome remodeling during the G2/MI transition was investigated by following relocalization or removal of the SC proteins SYCP1 and SYCP3 from the SC. The previously established short-term culture system (Handel et al. 1995; Wiltshire et al. 1995) was used and 200 spermatocytes were scored in each of three individual experiments (N = 600 spermatocytes). Removal of SYCP1 from the SC was scored

to follow disassembly of the central element and desynapsis, and relocalization of SYCP3 was scored to follow disassembly of the LEs of SCs. Desynapsis was the earliest event observed. At time zero (T0) nearly 80% of cells exhibited co-localization of SYCP1 and SYCP3 along autosomal SCs and in the paired XY pseudoautosomal region (Fig. 1a). In response to OA, the proportion of cells with uninterrupted SYCP1 signals decreased rapidly (Fig. 2a) as early as 0.5 hour after OA treatment ($p < 0.05$). By 3.0 hours after OA treatment, only about 10% of spermatocytes exhibited an uninterrupted and continuous SYCP1 signal along the SCs; these cells most likely represent early pachytene spermatocytes not yet competent to undergo the G2/MI transition in vitro (Cobb et al. 1999a; Handel et al. 1999). By this time, all other spermatocytes had entered the diplotene stage (marked by desynapsis) or reached the first meiotic metaphase (MI) (Fig. 1b,c). In diplotene spermatocytes (Fig. 1b), desynapsed regions labeled with anti-SYCP3 but not with anti-SYCP1, whereas in the synapsed regions of these spermatocytes, SYCP1 label co-localized with SYCP3 label. Identical antibody labeling patterns were observed in untreated late pachytene, diplotene and MI spermatocytes retrieved directly from testes (data not shown).

Phosphorylation of histone H3 on Ser10 is proposed to be the earliest event associated with chromosome condensation as cells progress into division phase. Previously we observed that histone H3 phosphorylation begins at centromeric heterochromatin after OA treatment (Cobb et al. 1999b). Here we used kinetic analysis to ask whether this occurs before, during or after OA-induced disassembly of the central elements of SCs. Surface-spread chromatin was double-labeled with antibodies against SYCP3 and histone H3 phosphorylated on Ser10 to follow both desynapsis and histone H3 phosphorylation. No spermatocytes with fully synapsed lateral SC elements were labeled with the antibody against phosphorylated histone H3, and labeling with this antibody was observed only in spermatocytes with desynapsed SYCP3-labeled LEs (Fig. 1d), indicating central element disassembly and entry into the diplotene stage. In some cells, patches of phosphorylated histone H3 signals were observed in heterochromatic regions (Fig. 1d), and in spermatocytes with histone H3 phosphorylation throughout the chromatin (Fig. 1e,f). Kinetic analysis of the temporal time-course of disappearance of SYCP1 signal and histone H3 phosphorylation confirmed that desynapsis is initiated before phosphorylation of histone H3 on Ser10 occurs. Disassembly of SYCP1 was observed at 0.5 hours of OA treatment (Fig. 2a), whereas the significant increase in the percentage of spermatocytes with phosphorylated histone H3 did not occur until 1.5 hours (30% of spermatocytes with phosphorylated histone H3) to 3.0 hours (80% of spermatocytes with phosphorylated histone H3) of incubation with OA (Fig. 2c), after which the increase became slower until at 5.0 hours of OA treatment, about 90% of cells exhibited histone H3 phosphorylation. Thus this kinetic analysis reveals that phosphorylation of histone H3 on Ser10 following OA treatment occurs after removal of SYCP1 from the SC, consistent previous observations on desynapsis, both in vitro and in vivo (Cobb et al. 1999b; Parra et al. 2003).

In contrast to the rapid onset of SYCP1 removal and phosphorylation of histone H3, relocalization of SYCP3, marking disassembly of SC LE, was not observed until 2.0 hours after initiation of OA treatment ($p < 0.01$) (Fig. 2b). Results of antibody labeling for both SYCP3 and histone H3 phosphorylated on Ser10 were consistent with this temporal analysis. As shown in Fig. 1d and e, some cells exhibited histone H3 phosphorylation, but had no signs of redistribution or removal of SYCP3, indicating that phosphorylation of histone H3 on Ser10 commenced before the initiation of SYCP3 loss. Thereafter, the frequency of cells with uninterrupted and linear SYCP3 labeling along the SC LEs steadily declined (Fig. 2b), during which time spermatocytes exhibited small patches of SYCP3 labeling located along the sister chromatids as previously reported (Parra et al. 2004;Prieto et al. 2001;Viera et al. 2003). By 5.0 hour culture with OA under our experimental conditions, most SYCP3 labeling disappeared from chromosome arms and accumulated in the centromeric regions (Fig. 1c, f), as observed in testicular MI spermatocytes (data not shown) and previously reported both in vivo and in

vitro (Dobson et al. 1994;Tarsounas et al. 1999), although a patchy and punctate labeling pattern for SYCP3 along chromosome arms was observed in some spread cells after 5.0 hour culture with OA. During this period, the frequency of MI spermatocytes, with fully condensed bivalents (Fig. 1g) increased to over 80% of the treated spermatocytes. In contrast to the autosomal chromosomes, the relocalization of SYCP3, similar to the in vivo situation, appeared to be delayed on sex chromosomes, where the SYCP3 signals persisted even in later stages, when the signals had become punctate or had disappeared in autosomes. This differential behavior suggests that different mechanisms and/or accessibility are involved in SYCP3 removal from autosomal LEs versus the sex chromosome axial elements (AEs). In the population of spermatocytes after 5.0 hour OA treatment, about 10% of the cells exhibited uninterrupted, linear co-localization of SYCP1 and SYCP3 labeling, indicating they were arrested at pachytene stage and presumably not competent to undergo the G2/MI transition.

Protein phosphorylation/dephosphorylation and other post-translational events are hallmarks of cell-cycle transitions. Indeed, it has been reported that SYCP1 possesses several potential target sites for protein kinases, and is phosphorylated in pachytene spermatocytes (Tarsounas et al. 1999). Therefore, we determined electrophoretic mobility of both of SYCP1 and SYCP3 in OA-treated spermatocytes. No band shifts were observed for either SYCP1 or SYCP3 after OA treatment on the western blots, suggesting no major modifications to the pachytene status of these proteins during the induced G2/MI in these conditions (Fig. 3).

Partial loss of meiosis-specific cohesin subunits coincides with SC disassembly during the G2/MI transition in vitro

Because meiosis-specific cohesins contribute to the integrity of meiotic LEs and the SC (Bannister et al. 2004; Revenkova et al. 2004; Xu et al. 2005), we examined the localization of two meiosis-specific cohesin subunits, REC8 and STAG3, during the OA-induced G2/MI transition. Both REC8 and STAG3 localized to the SC LEs in pachytene and early diplotene stages (Fig. 4a, b, c). The STAG3 signals, but not REC8 signals, were evenly distributed along the chromosomearms at pachytene and diplotene stages. During the induced G2/MI transition, STAG3 and REC8 exhibited dynamic re-localization that differed from SYCP3. In late diplonema, when autosomes are almost, but not completely, desynapsed, some bivalents had one or two SYCP3-labeled bridges, which may represent sites of chiasma formation, between the two axial elements, whereas REC8 and STAG3 were absent from these bridges (Fig. 4c), as previously observed in vivo (Eijpe et al. 2003; Prieto et al. 2001). By diakinesis/MI, when SYCP3 had re-localized from the chromosome arms to the centromeric regions, REC8 and STAG3 were only partially lost from chromosome arms, and were localized between sister chromatids (Fig. 4d, e) as in vivo (Eijpe et al. 2003; Prieto et al. 2001). This observation supports the concept that these proteins play a role in sister-chromatid cohesion, preventing premature sister-chromatid segregation during meiosis I(Eijpe et al. 2003).

CDK inhibition with BLI does not affect desynapsis or histone H3 phosphorylation during the G2/MI transition

MPF is a universal regulator of the prophase to metaphase transition in both mitosis and meiosis, and its action is inhibited by BLI (Furukawa et al. 1996; Nishio et al. 1996). We have previously shown that BLI inhibits the OA-induced G2/MI transition of spermatocytes, but not histone H3 phosphorylation on Ser10 (Cobb et al. 1999b); however, its effect on specific stages of SC disassembly was not known.

As shown in Fig. 5a, desynapsis and removal of SYCP1 began rapidly in spermatocytes after the treatment with either OA or OA + BLI and was almost completed after 3.0 hour treatment. Thus desynapsis is not sensitive to BLI. However, BLI inhibited the OA-induced relocalization of SYCP3 (Fig. 5b) and condensation and final compaction of bivalents (Fig. 5d). The pattern

of SYCP3 labeling in spermatocytes after OA + BLI treatment was similar to that in the solvent control, and in marked contrast to the OA group. By 5.0 hours after incubation, 92.4% and 91.1% spermatocytes in the solvent control and OA + BLI groups, respectively, exhibited uninterrupted SYCP3 labeling along the SC LEs, while only 17.7% spermatocytes in OA group failed to exhibit redistribution of SYCP3. Significant differences between OA and OA + BLI treatments were observed by 2.0 hour ($P < 0.05$). The concentration of BLI used (100 μM) inhibited histone H1 kinase activity (data not shown), as previously reported (Cobb et al. 1999b). As previously demonstrated by us, and as shown in Fig. 5c, the frequency of spermatocytes with histone H3 phosphorylated on Ser10 after OA treatment was unaffected by BLI. Together these findings suggest that BLI-sensitive CDKs are not responsible for SYCP1 removal from the SC or phosphorylation of histone H3 on Ser10, butthese kinases do play direct or indirect roles in SYCP3 removal and relocalization from the SC LEs and subsequent condensation of morphologically distinct bivalents.

ZM-sensitive AURKs affect histone H3 phosphorylation, compaction of bivalents, and disassembly of LEs, but not disassembly of the central element of the SC

Aurora kinases (AURKs) have histone H3 kinase activity, are involved in mitotic G2/M transition (Adams et al. 2001; Crosio et al. 2002; Goto et al. 1999; Scrittori et al. 2001), and are expressed in mouse spermatocytes in prophase of meiosis I (Kimmins et al. 2007; Parra et al. 2003; Tang et al. 2006). However, their precise role in steps of the G2/MI transition has not been directly demonstrated. We tested the effect of ZM, a small molecule inhibitor of AURK A and B (Ditchfield et al. 2003; Gadea and Ruderman 2005) on G2/MI processes in mouse spermatocytes.

We first determined that OA activates the AURKs in vitro. An in-gel kinase assay previously described was used to directly assess the phosphorylation activity of AURK on the AURK substrate thymus histone H3 (Crosio et al. 2002), and BSA as a control to assess specificity of AURKs. As shown in Fig. 6, the activity of AURKB in extracts of pachytene spermatocytes treated for 5.0 hours with OA increased 2.3 fold compared to extracts from control spermatocytes. Very little phosphorylation of the non-specific BSA substrate by AURKs was observed (data not shown), in agreement with the observations reported for somatic cells (Crosio et al. 2002). OA activation of AURK activity toward thymus histone H3 was inhibited by 5 μM ZM (Fig. 6a, lanes 3 and 5), and this dose was selected for further experiments.

OA-induced disassembly of the central element of the SC was not affected by ZM (Fig. 7a). In spermatocytes treated with either OA alone or OA + ZM, the process of desynapsis was completed within 3.0 hours; the frequency of cells with uninterrupted SYCP1 labeling decreased from 74.5% at T0 to 3.9% at T5 in OA group and from 73.8% to 5.6% in the OA + ZM group. This observation indicates that mechanisms other than ZM-sensitive AURKs promote disassembly of central element of SCs. However, OA-induced redistribution of SYCP3 from SC LEs was inhibited by ZM (Fig. 7b); thus this process depends on both BLI-sensitive CDKs and ZM-sensitive AURKs. Phosphorylation of histone H3 on Ser10 also was inhibited by ZM (Fig. 7c). In the presence of ZM, only 18.6% spermatocytes exhibited histone H3 phosphorylation 5.0 h after OA treatment, whereas in the absence of ZM, 81.1% cells exhibited histone H3 phosphorylation. These observations are consistent with similar effects of ZMon histone H3 phosphorylation during mitosis (Crosio et al. 2002). Thus, this inhibitor analysis reveals a meiotic role for AURKs in phosphorylation of histone H3 on Ser10, in relocalization of SYCP3 and in compaction and formation of morphologically distinct bivalents, but not in disassembly of the central element of SCs.

Discussion

The G2/MI transition: a step-wise process

The meiotic G2/MI transition involves disassembly of the SC structure, phosphorylation of histone H3, and remodeling of chromatin to bring about condensation of morphologically distinct bivalent chromosomes. To what degree these events are under common cell cycle control is not known. This regulation is difficult to analyze in vivo, in part because of the low number of spermatocytes undergoing the G2/MI transition at any specific time, but mostly because of the lack of germ-cell conditional mutations in relevant kinases and difficulty of inhibitor analyses in vivo. To circumvent these problems, we used mid-to late -pachytene mouse spermatocytes enriched from testes and induced the G2/MI transition by treatment with the phosphatase inhibitor OA, a system previously shown to faithfully reflect G2/MI transition events (Cobb et al. 1999b; Marcon and Moens 2003; Tarsounas et al. 1999; Wiltshire et al. 1995). Our kinetic and inhibitor analyses of events reveal that chromosome remodeling during the G2/MI transition is a differentially regulated step-wise process, diagrammatically represented in Fig. 8. The earliest visible step in the G2/MI transition is disassembly of the central element of the SC, marked by removal of SYCP1 from the SC, an event that defines diplonema, but separable in time and space from phosphorylation of histone H3 on Ser10 (Fig. 8). Subsequently SYCP3 and cohesins are removed from and/or relocalized in the LEs of the SC, concurrently with condensation and individualization of chiasmate bivalent chromosomes into their MI configuration (Fig. 8). Regulatory control over these events is unexpectedly complex. While it was previously assumed that MPF, the universal cell cycle regulator, might initiate the G2/MI transition, we show here that instead, it functions only in late G2/MI events: removal and relocalization of SYCP3 in the LE of the SC and the final condensation and formation of morphologically distinct bivalents (Fig. 8). We also find that AURKs play a role in meiotic histone H3 phosphorylation on Ser10, as well as later events of disassembly of the LE of the SC and condensation of bivalents (Fig. 8). Control over the initiating events of the G2/MI transition, specifically, disassembly of the central element of the SC, is not by either ZM-sensitive AURKs or BLI-sensitive CDKS (Fig. 8).

Initiating the G2/MI transition: disassembly of the central element of the SC and phosphorylation of histone H3

What initiates the exit from pachynema and transition into diplonema? It can be initiated in vitro by phosphatase inhibition, but is not mediated either by MAPKs (Inselman and Handel 2004)or cyclin A1 (Liu et al. 2000; Liu et al. 1998; Nickerson et al. 2007), or, surprisingly, by BLI-sensitive CDKs or ZM-sensitive AURKs, as we have shown here. It is likely that OA abrogates an endogenous inhibitor that maintains spermatocytes in pachynema, but what constitutes the inhibition process and what signals the onset of or mediates desynapsis either in vivo or in vitro is not known. Although in females, somatic cells control germ cell meiotic arrest, this is probably not the case for meiotic progress in males, as release of spermatocytes from their surrounding somatic cells does not stimulate meiotic progress (Wiltshire et al. 1995). A pachytene checkpoint, monitoring synapsis, has been proposed to regulate progress through meiotic prophase (Ashley et al. 2004; De Rooij and De Boer 2003; Odorisio et al. 1998), and may be involved in setting up competence to exit pachynema. This checkpoint is postulated to act at stage IV of the seminiferous epithelium, at approximately mid-pachynema and the time when MLH1/MLH3 foci appear on paired homologs; and indeed, this is also the time at which spermatocytes become competent to respond to OA by condensing chiasmate bivalent chromosomes (Cobb et al. 1999a). The proximal stimulus for the G2/MI transition may well be a signal transducer located in the SC and sensitive to completion of reciprocal recombination, perhaps an OA-sensitive phosphatase. Interestingly, the HSP7A2 chaperone is located within the SC (Allen et al. 1996), and its absence is associated with failure of spermatocytes to desynapse homologs (Dix et al. 1997), suggesting that this protein may be in

the chain of events initiating desynapsis. Phosphorylation of histone H3 on Ser10 is a marker for the onset of division phase in mitosis. Although it was previously known that histone H3 phosphorylation occurred in diplonema, this analysis established not only that it occurs after removal of SYCP1 from the SC but also that it is regulated differently than desynapsis. No spermatocytes with an intact SC central element were labeled for histone H3 phosphorylated on Ser10 and all spermatocytes with labeling for histone H3 phosphorylated on Ser10 exhibited desynapsis (Fig. 8). Thus the possibility exists that homolog desynapsis may lead to phosphorylation of histone H3. Histone H3 modification may also play a role in controlling subsequent condensation of bivalents and/or further dismantling of the SC (see below).

Disassembly of the LE of the SC and condensation of bivalents

SC disassembly is clearly a multi-step process, with desynapsis and removal of SYCP1 occurring hours before SYCP3 redistribution and removal both in vivo and in vitro after OA. The differential inhibitor sensitivity of disassembly of the central and lateral element of the SC indicates that control over dismantling the SC is complex. Very little is known about how orderly disassembly and relocalization of proteins from the SC is regulated, although at least some of the SYCP3 protein in the lateral axes relocalizes to the centromeric regions of chromosomes in the G2/MI transition (Dobson et al. 1994), and some persists in patches between sister chromatids (Parra et al. 2004; Prieto et al. 2001; Viera et al. 2003). The LEs are also marked by cohesin proteins, and we show here that the meiosis-specific REC8 and STAG3 cohesin subunits partially redistribute at approximately the same time as SYCP3 is removed from the LEs of the SC. Although SYCP3 is an integral component of the SC LEs; it is not sufficient for the assembly of meiotic LEs (Yuan et al. 2000; Yuan et al. 2002), and cohesins are required for the assembly of chromosomal axes (Eijpe et al. 2003; Page et al. 2006; Pelttari et al. 2001; Prieto et al. 2001; Revenkova et al. 2004). Thus it is possible that relocalization of the cohesins destabilizes the axes. As SYCP3 and cohesins are removed from the chromosomal axes, the chromatin loops are progressively compacted, resulting in the formation of condensed bivalents, maintained by chiasmata. Both cohesins and SYCP3 in the axes affect chromosome loop size and organization (Novak et al. 2008); furthermore condensin complexes are key elements for organization of meiotic chromosomes (Chan et al. 2004;Hagstrom and Meyer 2003; Tsai et al. 2008) and the condensin I complex localizes on mouse meiotic chromosomes (Viera et al. 2007). Both AURKs and phosphorylation of histone H3 may have critical roles for condensin function at this time. AURKB can target condensin I to mitotic chromatin and depletion of AURKB can result in loss of chromatin-bound histone H3 phosphorylation, with accompanying reduction of chromosomal targeting of condensin I in mitotic cells (Lipp et al. 2007; Takemoto et al. 2007). Thus phosphorylation of histone H3 on Ser10, mediated by AURKB, could be one mechanism contributing to final condensation of bivalents in spermatocytes. These results demonstrating impairment of chromosome condensation when AURKs are inhibited are in contrast to previous studies (Jelinkova and Kubelka 2006) suggesting that AURKB and phosphorylation of histone H3 on Ser10 may not be required for chromosome condensation in porcine oocytes treated by BLI. However, other studies on both pig (Bui et al. 2004)and mouse (Swain et al. 2007)oocytes have implicated a role for histone H3 phosphorylation on Ser10 in chromosome condensation during maturation. A recent study (Swain et al. 2008)reports a more direct test by treating mouse oocytes with ZM; the findings are similar to those reported here for spermatocytes, namely ZM inhibited phosphorylation of histone H3 on Ser10 and caused abnormalities in condensation of bivalents. Clearly, although there may be some species differences, roles of AURKS in histone H3 phosphorylation and chromosome condensation during the meiotic division phase are being resolved. In interesting similarity to ZM effects on spermatocytes, ZM treatment of oocytes (Swain et al. 2008)did not inhibit meiotic resumption (initiation of the G2/MI transition). Our data point to regulatory roles for both CDKs and AURKs in promoting final stages of chromosome compaction in

spermatocytes, but clearly further investigations will be required to reveal the specific roles of these regulators that contribute to SC disassembly and chromosome formation.

Differential and sequential kinase regulation of G2/MI events

MPF is a nearly universal regulator of events leading to chromosome condensation and individualization in mitotic and meiotic division phase. AURKs also play a role in the onset of the mitotic division phase. In the absence of suitable genetic models for unraveling the roles of these putative regulators, we targeted them with inhibitors. There are always caveats to be considered with this approach. One of the most important is the issue of whether the small molecule inhibitors reach their protein targets. Both BLI and ZM are known to traverse cell membranes. We also applied inhibitors before treating cells with the G2/MI transition-activating agent, OA. However, one cautionary note in interpretation of data is the possibility that efficacy of either BLI or ZM is greater after nuclear envelope breakdown. OA induces nuclear envelope breakdown in spermatocytes (Wiltshire et al. 1995), but the precise timing of this is not known. A second caveat is that inhibitors identify classes of proteins (e.g., CDKs or AURKs), but not usually specific proteins. Nonetheless, BLI and ZM effects allowed us to demonstrate differential regulation of steps in the G2/MI transition.

Inhibition of MPF abrogates OA-induced condensation of bivalents in the G2/MI transition as shown here and previously (Cobb et al. 1999a). Here we show that the CDK inhibitor BLI inhibits removal of SYCP3 from the SC, confirming the importance of CDK activity for disassembly of the SC. However, BLI did not inhibit OA-induced desynapsis; thus BLI-sensitive CDKs are not a “master regulator” of the G2/MI transition, implicating other regulators. Nonetheless, CDKs clearly have function in later stages of the G2/MI transition, and data reported here are consistent with genetic evidence implicating a role for CDKs. First, the HSP70-2 protein (now known as HSPA2) appears to be a molecular chaperone required for activation of CDC2A kinase in spermatocytes (Dix et al. 1997); and spermatocytes of mice with a knockout of the *Hspa2*gene arrest in meiotic prophase, failing to progress through the G2/MI transition (Dix et al. 1996; Dix et al. 1997). Second, spermatocytes of mice with a knockout of the gene encoding cyclin A1 (*Ccna1*) also fail to activate MPF and arrest at late diplotene (after desynapsis) but do not progress to MI (Liu et al. 2000; Liu et al. 1998; Nickerson et al. 2007). Together, these genetic data and our results here implicate MPF and, more broadly, CDKs in stages of the G2/MI transition following desynapsis, but not in desynapsis or phosphorylation of histone H3 on Ser10. Interestingly, paired bivalents in spermatocytes of mice deficient in HSP7A2 fail to undergo desynapsis (Dix et al. 1997), suggesting that HSPA2 may play a role in early events of the G2/MI transition that are unaffected by CDK inhibition.

What kinases other than BLI-sensitive CDKs might play a role in the G2/MI transition? AURKs, especially AURKB, are implicated in the phosphorylation of histone H3 on Ser10 (Carmena and Earnshaw 2003), and are present in male germ cells (Kimmins et al. 2007; Parra et al. 2003)at the right time and place to be involved in the G2/MI transition. AURKB co-localizes with phosphorylated histone H3 in late meiotic cells (Kimmins et al. 2007). Expression of a kinase-inactive AURKB causes multiple spermatogenic abnormalities, including abnormal germ cell – somatic cell associations in the testis (Kimmins et al. 2007); these multiple abnormalities precluded determination of precise roles for AURKB in the meiotic division phase. We show here that ZM inhibition of AURKs inhibits OA-induced phosphorylation of histone H3 on Ser10, as well as removal of SYCP3 from LEs and condensation and formation of morphologically distinct bivalents. Meiotic function for AURKs in phosphorylation of histone H3 on Ser10 presented here is consistent with its activity in mitosis and ZM effects on chromosome individualization and disassembly of the SC LEs implicate either a direct role for AURKs in these processes or an indirect role via

phosphorylated histone H3, which may serve to recruit condensins to the chromatin. However, inhibition of AURKs with ZM did not impede desynapsis and removal of SYCP1 from the SC at the onset of the OA-induced diplotene stage, providing evidence that these events are controlled by other positive or negative regulators of the G2/MI transition, including an OA-sensitive phosphatase.

In conclusion, kinetic and inhibitor analysis of the G2/MI transition reveals distinct, sequential and separable steps in the G2/MI transition under differential control and that MPF, the universal cell cycle regulator, does not control initiation of the G2/MItransition (Fig. 8). Both final stages of condensation of bivalents and final disassembly of the SC are regulated, directly or indirectly, by both CDKs and AURKs, and AURKs mediate phosphorylation of histone H3 on Ser10 at an early stage of the G2/MI transition (Fig. 8). Finally, neither BLI-sensitive CDKs nor ZM-sensitive AURKs regulate the signaling pathway and mechanisms that initiate desynapsis and removal of SYCP1 from the SC; thus the key players in this critical step of meiosis are yet to be discovered.

Acknowledgments

We thank Dr. Christa Heyting for providing antibodies to SYCP1 and REC8. We are grateful to Drs. John Eppig, Sophie La Salle, Laura Reinholdt and Lindsay Shopland for providing critical comments on the manuscript. We wish to thank Heather Lothrop for maintaining the mice, and Dr. Jim Denegre and Bobbi-Jo Shirley of the biological imaging facility for assistance. This work was supported by a grant from the NIH to MAH (HD33816) and a Cancer Center Core Grant to The Jackson Laboratory (CA34196).

References

Adams RR, Maiato H, Earnshaw WC, Carmena M. Essential roles of Drosophila inner centromere protein (INCENP) and aurora B in histone H3 phosphorylation, metaphase chromosome alignment, kinetochore disjunction, and chromosome segregation. J Cell Biol 2001;153:865–880. [PubMed: 11352945]

Allen JW, Dix DJ, Collins BW, Merrick BA, He C, Selkirk JK, Poorman-Allen P, Dresser ME, Eddy EM. Hsp70-2 is part of the synaptonemal complex in mouse and hamster spermatocytes. Chromosoma 1996;104:414–421. [PubMed: 8601336]

Arlot-Bonnemains Y, Klotzbucher A, Giet R, Uzbekov R, Bihan R, Prigent C. Identification of a functional destruction box in the *Xenopus laevis* aurora -A kinase pEg2. FEBS Lett 2001;508:149–152. [PubMed: 11707286]

Ashley T, Gaeth AP, Creemers LB, Hack AM, De Rooij DG. Correlation of meiotic events in testis sections and microspreads of mouse spermatocytes relative to the mid-pachytene checkpoint. Chromosoma 2004;113:126–136. [PubMed: 15338235]

Bannister LA, Reinholdt LG, Munroe RJ, Schimenti JC. Positional cloning and characterization of mouse *mei8*, a disrupted allelle of the meiotic cohesin Rec8. Genesis 2004;40:184–194. [PubMed: 15515002]

Bellve AR. Purification, culture, and fractionation of spermatogenic cells. Methods Enzymol 1993;225:84–113. [PubMed: 8231890]

Belmont AS. Mitotic chromosome structure and condensation. Curr Opin Cell Biol 2006;18:632–638. [PubMed: 17046228]

Bolcun-Filas E, Costa Y, Speed R, Taggart M, Benavente R, De Rooij DG, Cooke HJ. *Syce2*is required for synaptonemal complex assembly, double strand break repair, and homologous recombination. J Cell Biol 2007;176:741–747. [PubMed: 17339376]

Bui HT, Yamaoka E, Miyano T. Involvement of histone H3 (ser10) phosphorylation in chromosome condensation without Cdc2 kinase and mitogen-activated protein kinase activation in pig oocytes. Biol Reprod 2004;70:1843–1851. [PubMed: 14960481]

Carmena M, Earnshaw WC. The cellular geography of aurora kinases. Nat Rev Mol Cell Biol 2003;4:842–854. [PubMed: 14625535]

Chan RC, Severson AF, Meyer BJ. Condensin restructures chromosomes in preparation for meiotic divisions. J Cell Biol 2004;167:613–625. [PubMed: 15557118]

Chieffi P, Troncone G, Caleo A, Libertini S, Linardopoulos S, Tramontano D, Portella G. Aurora B expression in normal testis and seminomas. J Endocrinol 2004;181:263–270. [PubMed: 15128274]

Cobb J, Cargile B, Handel MA. Acquisition of competence to condense metaphase I chromosomes during spermatogenesis. Dev Biol 1999a;205:49–64. [PubMed: 9882497]

Cobb J, Reddy RK, Park C, Handel MA. Analysis of expression and function of topoisomerase I and II during meiosis in male mice. Mol Reprod Dev 1997;46:489–498. [PubMed: 9094096]

Cobb J, Miyaike M, Kikuchi A, Handel MA. Meiotic events at the centromeric heterochromatin: Histone H3 phosphorylation, topoisomerase II alpha localization and chromosome condensation. Chromosoma 1999b;108:412–425. [PubMed: 10654080]

Colledge WH, Carlton MB, Udy GB, Evans MJ. Disruption of c-mos causes parthenogenetic development of unfertilized mouse eggs. Nature 1994;370:65–68. [PubMed: 8015609]

Costa Y, Speed R, Ollinger R, Alsheimer M, Semple CA, Gautier P, Maratou K, Novak I, Hoog C, Benavente R, Cooke HJ. Two novel proteins recruited by synaptonemal complex protein 1 (SYCP1) are at the centre of meiosis. J Cell Sci 2005;118:2755–2762. [PubMed: 15944401]

Crane R, Gadea B, Littlepage L, Wu H, Ruderman JV. Aurora A, meiosis and mitosis. Biol Cell 2004;96:215–229. [PubMed: 15182704]

Crosio C, Fimia GM, Loury R, Kimura M, Okano Y, Zhou H, Sen S, Allis CD, Sassone-Corsi P. Mitotic phosphorylation of histone H3: Spatio-temporal regulation by mammalian aurora kinases. Mol Cell Biol 2002;22:874–885. [PubMed: 11784863]

de Rooij DG, de Boer P. Specific arrests of spermatogenesis in genetically modified and mutant mice. Cytogenet Genome Res 2003;103:267–276. [PubMed: 15051947]

de Vries FA, de Boer E, van den Bosch M, Baarends WM, Ooms M, Yuan L, Liu JG, van Zeeland AA, Heyting C, Pastink A. Mouse SYCP1 functions in synaptonemal complex assembly, meiotic recombination, and XY body formation. Genes Dev 2005;19:1376–1389. [PubMed: 15937223]

Ditchfield C, Johnson VL, Tighe A, Ellston R, Haworth C, Johnson T, Mortlock A, Keen N, Taylor SS. Aurora B couples chromosome alignment with anaphase by targeting BubR1, Mad2, and Cenp-E to kinetochores. J Cell Biol 2003;161:267–280. [PubMed: 12719470]

Dix DJ, Allen JW, Collins BW, Mori C, Nakamura N, Poorman-Allen P, Goulding EH, Eddy EM. Targeted gene disruption of Hsp70-2 results in failed meiosis, germ cell apoptosis, and male infertility. Proc Natl Acad Sci U S A 1996;93:3264–3268. [PubMed: 8622925]

Dix DJ, Allen JW, Collins BW, Poorman-Allen P, Mori C, Blizard DR, Brown PR, Goulding EH, Strong BD, Eddy EM. HSP70-2 is required for desynapsis of synaptonemal complexes during meiotic prophase in juvenile and adult mouse spermatocytes. Development 1997;124:4595–4603. [PubMed: 9409676]

Dobson MJ, Pearlman RE, Karaiskakis A, Spyropoulos B, Moens PB. Synaptonemal complex proteins: Occurrence, epitope mapping and chromosome disjunction. J Cell Sci 1994;107:2749–2760. [PubMed: 7876343]

Eaker S, Pyle A, Cobb J, Handel MA. Evidence for meiotic spindle checkpoint from analysis of spermatocytes from Robertsonian-chromosome heterozygous mice. J Cell Sci 2001;114:2953–2965. [PubMed: 11686299]

Eijpe M, Heyting C, Gross B, Jessberger R. Association of mammalian SMC1 and SMC3 proteins with meiotic chromosomes and synaptonemal complexes. J Cell Sci 2000;113:673–682. [PubMed: 10652260]

Eijpe M, Offenberg H, Jessberger R, Revenkova E, Heyting C. Meiotic cohesin Rec8 marks the axial elements of rat synaptonemal complexes before cohesins SMC1beta and SMC3. J Cell Biol 2003;160:657–670. [PubMed: 12615909]

Evans EP, Breckon G, Ford CE. An air-drying method for meiotic preparations from mammalian testes. Cytogenetics 1964;15:289–294. [PubMed: 14248459]

Furukawa Y, Iwase S, Terui Y, Kikuchi J, Sakai T, Nakamura M, Kitagawa S, Kitagawa M. Transcriptional activation of the Cdc2 gene is associated with Fas-induced apoptosis of human hematopoietic cells. J Biol Chem 1996;271:28469–28477. [PubMed: 8910474]

Gadea BB, Ruderman JV. Aurora kinase inhibitor ZM447439 blocks chromosome-induced spindle assembly, the completion of chromosome condensation, and the establishment of the spindle integrity checkpoint in *Xenopus* egg extracts. Mol Biol Cell 2005;16:1305–1318. [PubMed: 15616188]

Godet M, Thomas A, Rudkin BB, Durand P. Developmental changes in cyclin B1 and cyclin-dependent kinase 1 (CDK1) levels in the different populations of spermatogenic cells of the post-natal rat testis. Eur J Cell Biol 2000;79:816–823. [PubMed: 11139145]

Godet M, Damestoy A, Mouradian S, Rudkin BB, Durand P. Key role for cyclin-dependent kinases in the first and second meiotic divisions of rat spermatocytes. Biol Reprod 2004;70:1147–1152. [PubMed: 14695906]

Goto H, Tomono Y, Ajiro K, Kosako H, Fujita M, Sakurai M, Okawa K, Iwamatsu A, Okigaki T, Takahashi T, Inagaki M. Identification of a novel phosphorylation site on histone H3 coupled with mitotic chromosome condensation. J Biol Chem 1999;274:25543–25549. [PubMed: 10464286]

Hagstrom KA, Meyer BJ. Condensin and cohesin: More than chromosome compactor and glue. Nat Rev Genet 2003;4:520–534. [PubMed: 12838344]

Hamer G, Gell K, Kouznetsova A, Novak I, Benavente R, Hoog C. Characterization of a novel meiosis-specific protein within the central element of the synaptonemal complex. J Cell Sci 2006;119:4025–4032. [PubMed: 16968740]

Handel MA, Caldwell KA, Wiltshire T. Culture of pachytene spermatocytes for analysis of meiosis. Dev Genet 1995;16:128–139. [PubMed: 7736663]

Handel MA, Cobb J, Eaker S. What are the spermatocyte's requirements for successful meiotic division? J Exp Zool 1999;285:243–250. [PubMed: 10497323]

Hashimoto N, Watanabe N, Furuta Y, Tamemoto H, Sagata N, Yokoyama M, Okazaki K, Nagayoshi M, Takeda N, Ikawa Y, et al. Parthenogenetic activation of oocytes in c-mos-deficient mice. Nature 1994;370:68–71. [PubMed: 8015610]

Hendzel MJ, Wei Y, Mancini MA, Van Hooser A, Ranalli T, Brinkley BR, Bazett-Jones DP, Allis CD. Mitosis-specific phosphorylation of histone H3 initiates primarily within pericentromeric heterochromatin during G2 and spreads in an ordered fashion coincident with mitotic chromosome condensation. Chromosoma 1997;106:348–360. [PubMed: 9362543]

Heyting C, Dietrich AJ, Redeker EJ, Vink AC. Structure and composition of synaptonemal complexes, isolated from rat spermatocytes. Eur J Cell Biol 1985;36:307–314. [PubMed: 3996433]

Heyting C, Moens PB, van Raamsdonk W, Dietrich AJ, Vink AC, Redeker EJ. Identification of two major components of the lateral elements of synaptonemal complexes of the rat. Eur J Cell Biol 1987;43:148–154. [PubMed: 3552678]

Hunter N. Synaptonemal complexities and commonalities. Mol Cell 2003;12:533 –535. [PubMed: 14527398]

Inselman A, Handel MA. Mitogen-activated protein kinase dynamics during the meiotic G2/MI transition of mouse spermatocytes. Biol Reprod 2004;71:570–578. [PubMed: 15084480]

Jelinkova L, Kubelka M. Neither aurora B activity nor histone H3 phosphorylation is essential for chromosome condensation during meiotic maturation of porcine oocytes. Biol Reprod 2006;74:905–912. [PubMed: 16452462]

Kimmins S, Crosio C, Kotaja N, Hirayama J, Monaco L, Hoog C, van Duin M, Gossen JA, Sassone-Corsi P. Differential functions of the aurora-B and aurora-C kinases in mammalian spermatogenesis. Mol Endo 2007;21:726–739.

Kouznetsova A, Novak I, Jessberger R, Hoog C. SYCP2 and SYCP3 are required for cohesin core integrity at diplotene but not for centromere cohesion at the first meiotic division. J Cell Sci 2005;118:2271–2278. [PubMed: 15870106]

Lipp JJ, Hirota T, Poser I, Peters JM. Aurora B controls the association of condensin I but not condensin II with mitotic chromosomes. J Cell Sci 2007;120:1245–1255. [PubMed: 17356064]

Liu D, Liao C, Wolgemuth DJ. A role for cyclin A1 in the activation of MPF and G2-M transition during meiosis of male germ cells in mice. Dev Biol 2000;224:388–400. [PubMed: 10926775]

Liu D, Matzuk MM, Sung WK, Guo Q, Wang P, Wolgemuth DJ. Cyclin A1 is required for meiosis in the male mouse. Nat Genet 1998;20:377–380. [PubMed: 9843212]

Marcon E, Moens P. MLH1p and MLH3p localize to precociously induced chiasmata of okadaic-acid-treated mouse spermatocytes. Genetics 2003;165:2283–2287. [PubMed: 14704203]

Meuwissen RL, Offenberg HH, Dietrich AJ, Riesewijk A, van Iersel M, Heyting C. A coiled-coil related protein specific for synapsed regions of meiotic prophase chromosomes. EMBO J 1992;11:5091–5100. [PubMed: 1464329]

Moens PB. Histones H1 and H4 of surface-spread meiotic chromosomes. Chromosoma 1995;104:169–174. [PubMed: 8529456]

Nickerson HD, Joshi A, Wolgemuth DJ. Cyclin A1-deficient mice lack histone H3 serine 10 phosphorylation and exhibit altered aurora B dynamics in late prophase of male meiosis. Dev Biol 2007;306:725–735. [PubMed: 17498682]

Nishio K, Ishida T, Arioka H, Kurokawa H, Fukuoka K, Nomoto T, Fukumoto H, Yokote H, Saijo N. Antitumor effects of butyrolactone I, a selective Cdc2 kinase inhibitor, on human lung cancer cell lines. Anticancer Res 1996;16:3387–3395. [PubMed: 9042196]

Novak I, Wang H, Revenkova E, Jessberger R, Scherthan H, Hoog C. Cohesin SMC1beta determines meiotic chromatin axis loop organization. J Cell Biol 2008;180:83–90. [PubMed: 18180366]

Odorisio T, Rodriguez TA, Evans EP, Clarke AR, Burgoyne PS. The meiotic checkpoint monitoring synapsis eliminates spermatocytes via p53-independent apoptosis. Nat Genet 1998;18:257–261. [PubMed: 9500548]

Offenberg HH, Schalk JA, Meuwissen RL, van Aalderen M, Kester HA, Dietrich AJ, Heyting C. Scp2: A major protein component of the axial elements of synaptonemal complexes of the rat. Nucleic Acids Res 1998;26:2572–2579. [PubMed: 9592139]

Page J, de la Fuente R, Gomez R, Calvente A, Viera A, Parra MT, Santos JL, Berrios S, Fernandez-Donoso R, Suja JA, Rufas JS. Sex chromosomes, synapsis, and cohesins: A complex affair. Chromosoma 2006;115:250–259. [PubMed: 16544151]

Parra MT, Viera A, Gomez R, Page J, Carmena M, Earnshaw WC, Rufas JS, Suja JA. Dynamic relocalization of the chromosomal passenger complex proteins inner centromere protein (INCENP) and aurora-B kinase during male mouse meiosis. J Cell Sci 2003;116:961–974. [PubMed: 12584241]

Parra MT, Viera A, Gomez R, Page J, Benavente R, Santos JL, Rufas JS, Suja JA. Involvement of the cohesin Rad21 and SCP3 in monopolar attachment of sister kinetochores during mouse meiosis I. J Cell Sci 2004;117:1221–1234. [PubMed: 14970259]

Pelttari J, Hoja MR, Yuan L, Liu JG, Brundell E, Moens P, Santucci-Darmanin S, Jessberger R, Barbero JL, Heyting C, Hoog C. A meiotic chromosomal core consisting of cohesin complex proteins recruits DNA recombination proteins and promotes synapsis in the absence of an axial element in mammalian meiotic cells. Mol Cell Biol 2001;21:5667–5677. [PubMed: 11463847]

Pezzi N, Prieto I, Kremer L, Perez Jurado LA, Valero C, Del Mazo J, Martinez AC, Barbero JL. STAG3, a novel gene encoding a protein involved in meiotic chromosome pairing and location of STAG3-related genes flanking the Williams-Beuren syndrome deletion. FASEB J 2000;14:581–592. [PubMed: 10698974]

Prieto I, Suja JA, Pezzi N, Kremer L, Martinez AC, Rufas JS, Barbero JL. Mammalian STAG3 is a cohesin specific to sister chromatid arms in meiosis I. Nat Cell Biol 2001;3:761–766. [PubMed: 11483963]

Revenkova E, Eijpe M, Heyting C, Gross B, Jessberger R. Novel meiosis-specific isoform of mammalian SMC1. Mol Cell Biol 2001;21:6984–6998. [PubMed: 11564881]

Revenkova E, Eijpe M, Heyting C, Hodges CA, Hunt PA, Liebe B, Scherthan H, Jessberger R. Cohesin SMC1 beta is required for meiotic chromosome dynamics, sister chromatid cohesion and DNA recombination. Nat Cell Biol 2004;6:555–562. [PubMed: 15146193]

Scrittori L, Hans F, Angelov D, Charra M, Prigent C, Dimitrov S. pEg2 aurora-A kinase, histone H3 phosphorylation, and chromosome assembly in *Xenopus* egg extract. J Biol Chem 2001;276:30002–30010. [PubMed: 11402032]

Sette C, Barchi M, Bianchini A, Conti M, Rossi P, Geremia R. Activation of the mitogen-activated protein kinase ERK1 during meiotic progression of mouse pachytene spermatocytes. J Biol Chem 1999;274:33571–33579. [PubMed: 10559244]

Swain JE, Ding J, Wu J, Smith GD. Regulation of spindle and chromatin dynamics during early and late stages of oocyte maturation by aurora kinases. Mol Hum Reprod. 2008 March 18;Epub ahead of print

Swain JE, Ding J, Brautigan DL, Villa-Moruzzi E, Smith GD. Proper chromatin condensation and maintenance of histone H3 phosphorylation during mouse oocyte meiosis requires protein phosphatase activity. Biol Reprod 2007;76:628–638. [PubMed: 17182892]

Swedlow JR, Hirano T. The making of the mitotic chromosome: Modern insights into classical questions. Mol Cell 2003;11:557–569. [PubMed: 12667441]

Takemoto A, Murayama A, Katano M, Urano T, Furukawa K, Yokoyama S, Yanagisawa J, Hanaoka F, Kimura K. Analysis of the role of aurora B on the chromosomal targeting of condensin I. Nucleic Acids Res 2007;35:2403–2412. [PubMed: 17392339]

Tang CJ, Lin CY, Tang TK. Dynamic localization and functional implications of aurora-C kinase during male mouse meiosis. Dev Biol 2006;290:398–410. [PubMed: 16386730]

Tarsounas M, Pearlman RE, Moens PB. Meiotic activation of rat pachytene spermatocytes with okadaic acid: The behaviour of synaptonemal complex components SYN1/SCP1 and COR1/SCP3. J Cell Sci 1999;112:423–434. [PubMed: 9914155]

Tsai CJ, Mets DG, Albrecht MR, Nix P, Chan A, Meyer BJ. Meiotic crossover number and distribution are regulated by a dosage compensation protein that resembles a condensin subunit. Genes Dev 2008;22:194–211. [PubMed: 18198337]

Viera A, Parra MT, Page J, Santos JL, Rufas JS, Suja JA. Dynamic relocation of telomere complexes in mouse meiotic chromosomes. Chromosome Res 2003;11:797–807. [PubMed: 14712865]

Viera A, Gomez R, Parra MT, Schmiesing JA, Yokomori K, Rufas JS, Suja JA. Condensin I reveals new insights on mouse meiotic chromosome structure and dynamics. PLoS ONE 2007;2:e783. [PubMed: 17712430]

von Wettstein D. The synaptonemal complex and genetic segregation. Symp Soc Exp Biol 1984;38:195–231. [PubMed: 6545723]

Wiltshire T, Park C, Caldwell KA, Handel MA. Induced premature G2/M-phase transition in pachytene spermatocytes includes events unique to meiosis. Dev Biol 1995;169:557–567. [PubMed: 7781899]

Wooten MW. In-gel kinase assay as a method to identify kinase substrates. Sci STKE 2002:PL15. [PubMed: 12372853]

Xu H, Beasley MD, Warren WD, van der Horst GT, McKay MJ. Absence of mouse REC8 cohesin promotes synapsis of sister chromatids in meiosis. Dev Cell 2005;8:949–961. [PubMed: 15935783]

Yang F, De La Fuente R, Leu NA, Baumann C, McLaughlin KJ, Wang PJ. Mouse SYCP2 is required for synaptonemal complex assembly and chromosomal synapsis during male meiosis. J Cell Biol 2006;173:497–507. [PubMed: 16717126]

Yao LJ, Sun QY. Characterization of aurora-A in porcine oocytes and early embryos implies its functional roles in the regulation of meiotic maturation, fertilization and cleavage. Zygote 2005;13:23–30. [PubMed: 15984158]

Yao LJ, Zhong ZS, Zhang LS, Chen DY, Schatten H, Sun QY. Aurora-A is a critical regulator of microtubule assembly and nuclear activity in mouse oocytes, fertilized eggs, and early embryos. Biol Reprod 2004;70:1392–1399. [PubMed: 14695913]

Yuan L, Liu JG, Zhao J, Brundell E, Daneholt B, Hoog C. The murine SCP3 gene is required for synaptonemal complex assembly, chromosome synapsis, and male fertility. Mol Cell 2000;5:73–83. [PubMed: 10678170]

Yuan L, Liu JG, Hoja MR, Wilbertz J, Nordqvist K, Hoog C. Female germ cell aneuploidy and embryo death in mice lacking the meiosis-specific protein SCP3. Science 2002;296:1115–1118. [PubMed: 12004129]

Zickler D, Kleckner N. Meiotic chromosomes: Integrating structure and function. Annu Rev Genet 1999;33:603–754. [PubMed: 10690419]

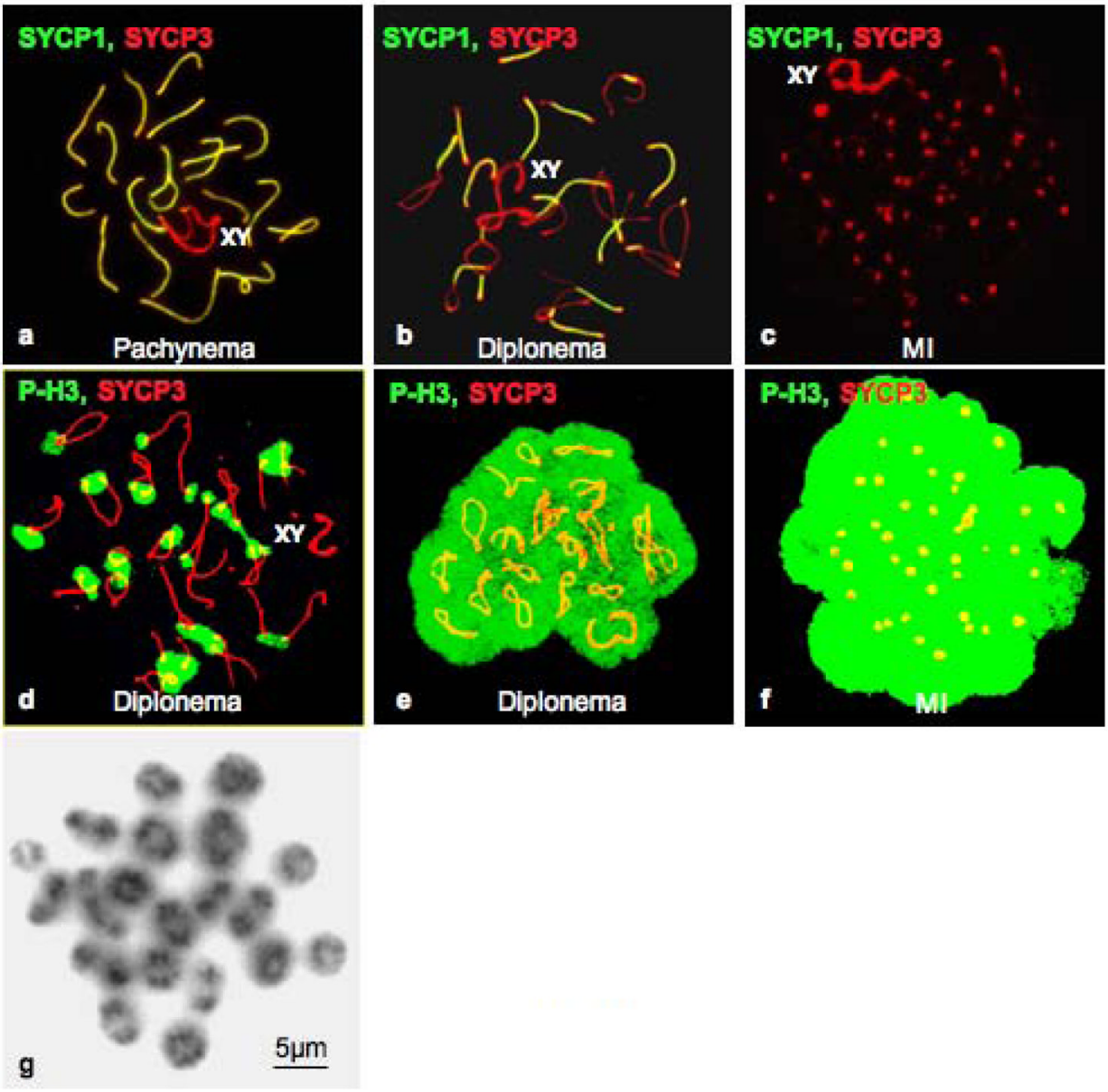

Figure 1.

Dynamics of SYCP1, SYCP3, phosphorylation of histone H3 on Ser10 labeling, and condensation of bivalents during the G2/MI transition in vitro. Labeling patterns of SYCP1 (green) and SYCP3 (red) are shown in pachynema (**a**), diplonema (**b**), and MI (**c**) during the OA-induced G2/MI transition in vitro. Different labeling patterns during the G2/MI transition in vitro for histone H3 phosphorylated on Ser10 (green) in diplonema and MI are shown in panels **d–f**. Respective stages of the cells were determined by the pattern of SYCP3 labeling (red). The sex bivalent is indicated as XY. Panel **g**. Giemsa staining reveals condensed bivalents in MI spermatocytes 5.0 hours after OA treatment.

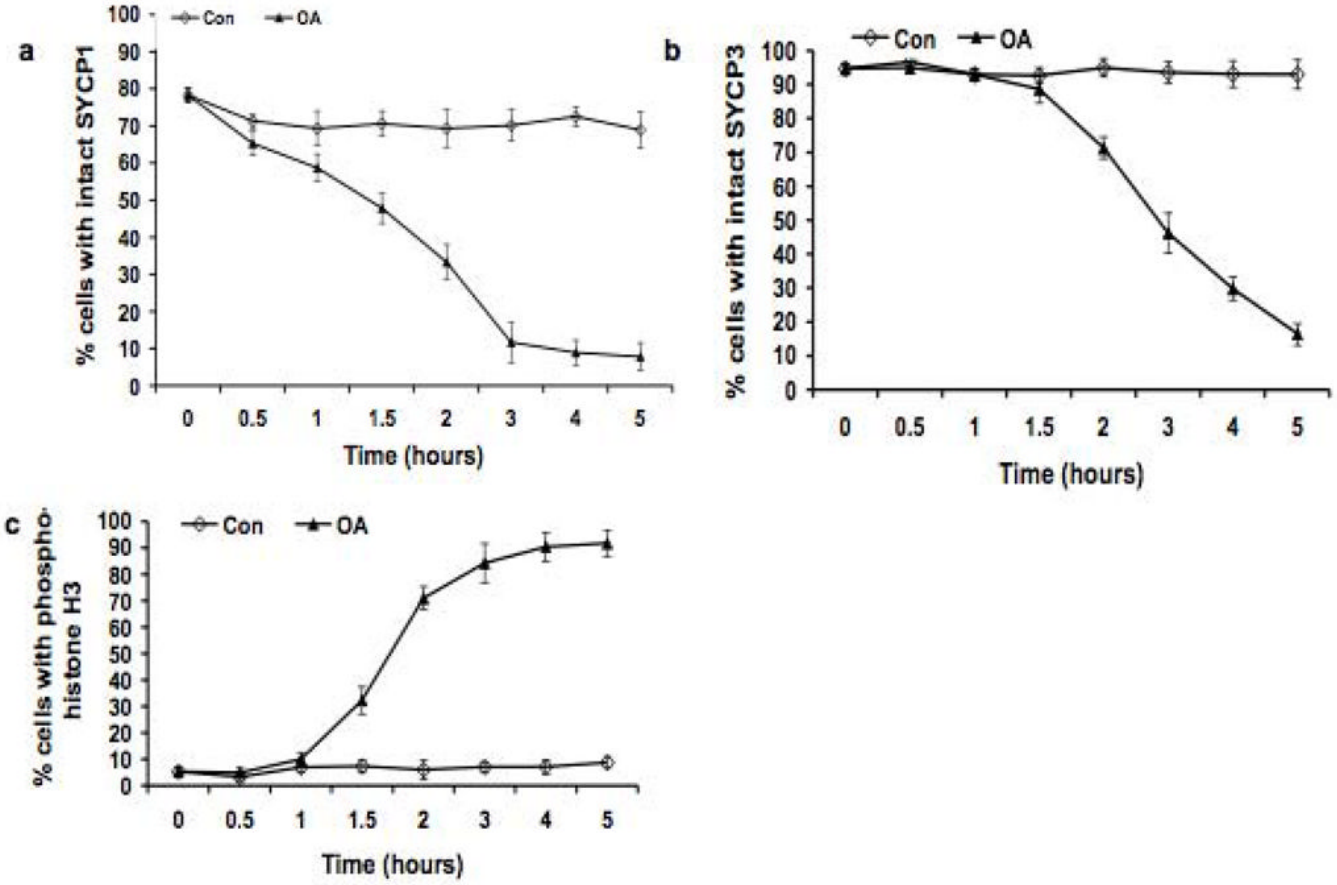

Figure 2.

Kinetic analysis of the dynamics of SYCP1, SYCP3 and appearance of histone H3 phosphorylated on Ser10 during the OA-induced G2/MI transition in vitro. The frequency (%) of cells with uninterrupted (intact), pachytene-like signal for SYCP1 and SYCP3 was scored. 200 cells were scored for SYCP1 and SYCP3, and the experiment was repeated three times (a total of 600 cells scored); 200 cells were scored for histone H3 phosphorylated on Ser10, and the experiment was repeated three times (a total of 600 cells scored). ◇: untreated control (Con) cells; ▲: cells treated with 5 μMOA (OA). Data are presented as means ± SEM.

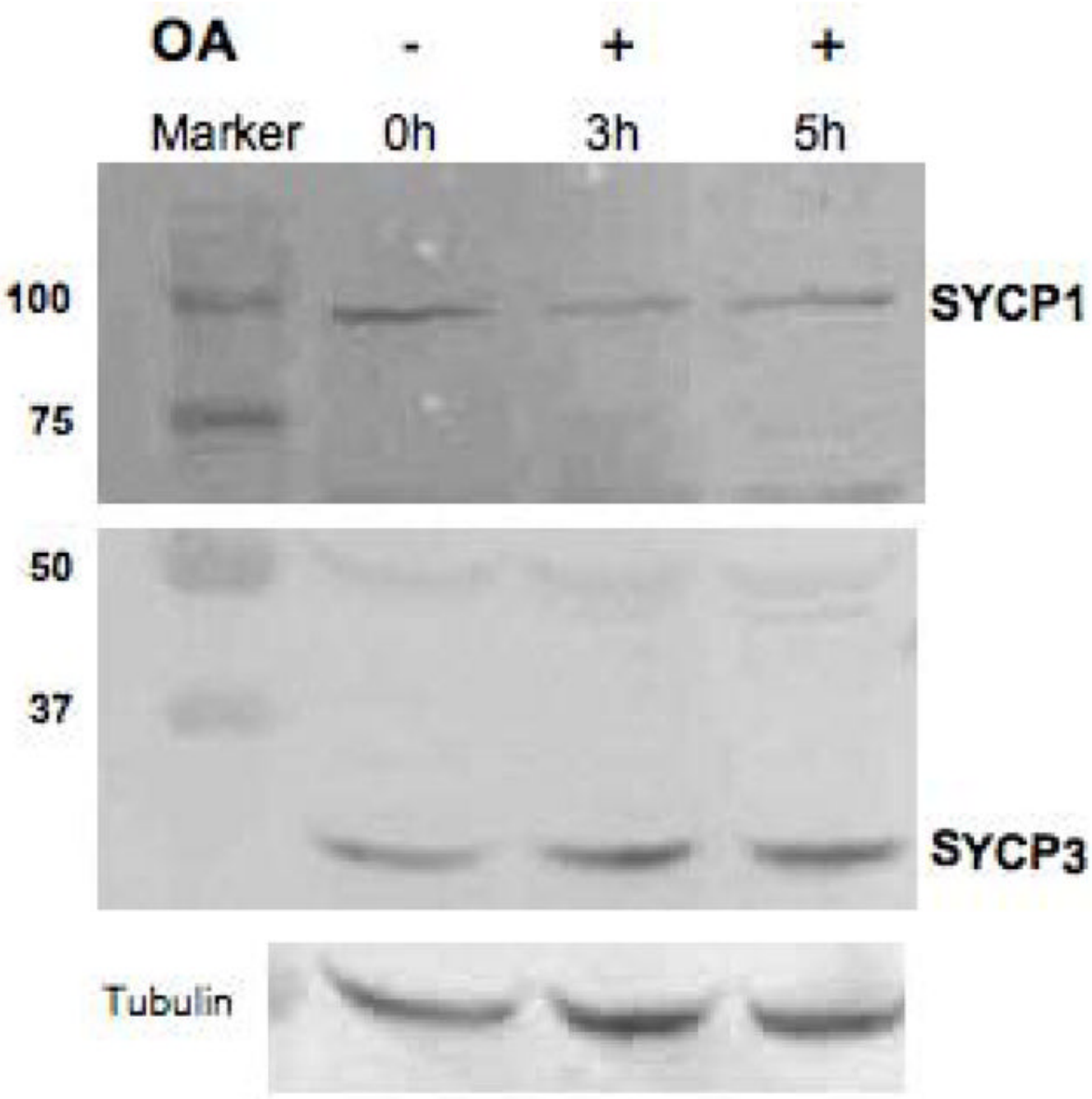

Figure 3.
Western blot detection of SYCP1 (top panel) and SYCP3 (middle panel) during the G2/MI transition in vitro (+ and − OA, 5 μM), with α-tubulin used as a loading control (bottom panel). This analysis was repeated three times and a typical result is shown here.

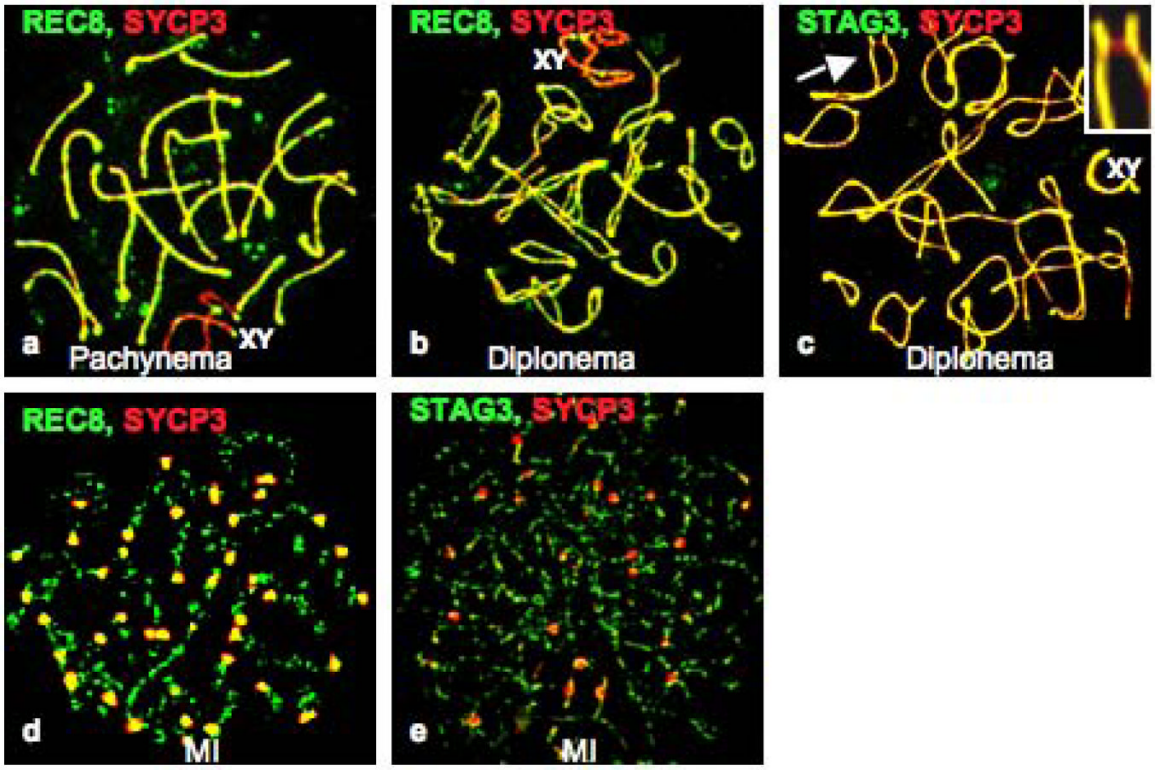

Figure 4.

Relocalization of the meiosis-specific cohesin subunits during the G2/MI transition in vitro. Panel **a** shows the relative localization of REC8 (green) and SYCP3 (red) in pachynema, and **b** shows their localization in diplonema. Panel **c** shows the absence of STAG3 (green, arrow) in an inter-homolog bridge labeled with anti-SYCP3 (red; arrow and enlargement in inset). The sex bivalent is indicated as XY. Panels **d** and **e** show the accumulation of SYCP3 (red) at centromeres at MI, when both REC8 (**d**, green) and STAG3 (e, green) are still present on chromosome arms.

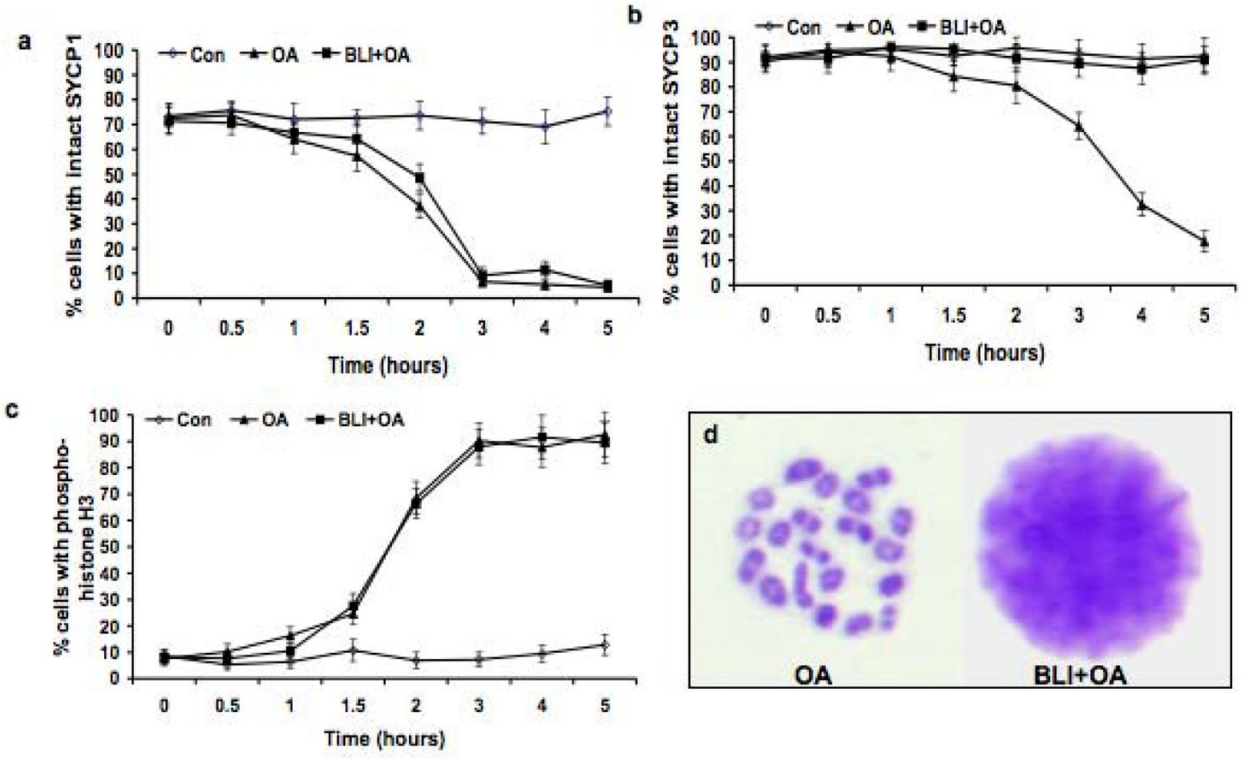

Figure 5.

Effects of BLI on the disassembly of the SCs and histone H3 phosphorylation on Ser10, and on condensation of bivalents. Panel **a** shows the dynamics of the removal of SYCP1 (desynapsis) in each experimental group. Panel **b** shows the removal of SYCP3 from the SC LEs in each experimental group. Panel **c** shows the increase in histone H3 phosphorylated on Ser10 in each experimental group. The frequency (%) of cells with uninterrupted (intact), pachytene-like signal for SYCP1 and SYCP3 was scored. 200 cells were scored for SYCP1 and SYCP3, and the experiment was repeated three times (a total of 600 cells scored); 200 cells were scored for phosphorylated histone H3, and the experiment was repeated three times (a total of 600 cells scored). ◇: untreated control (Con) cells; ▲: cells treated with 5 μMOA - treated (OA); ■ cells treated with 100 μM BLI + 5 μMOA (BLI + OA). The data are presented as means ± SEM. Panel d shows the patterns of chromatin condensation in OA-treated (left) and OA + BLI-treated spermatocytes (right).

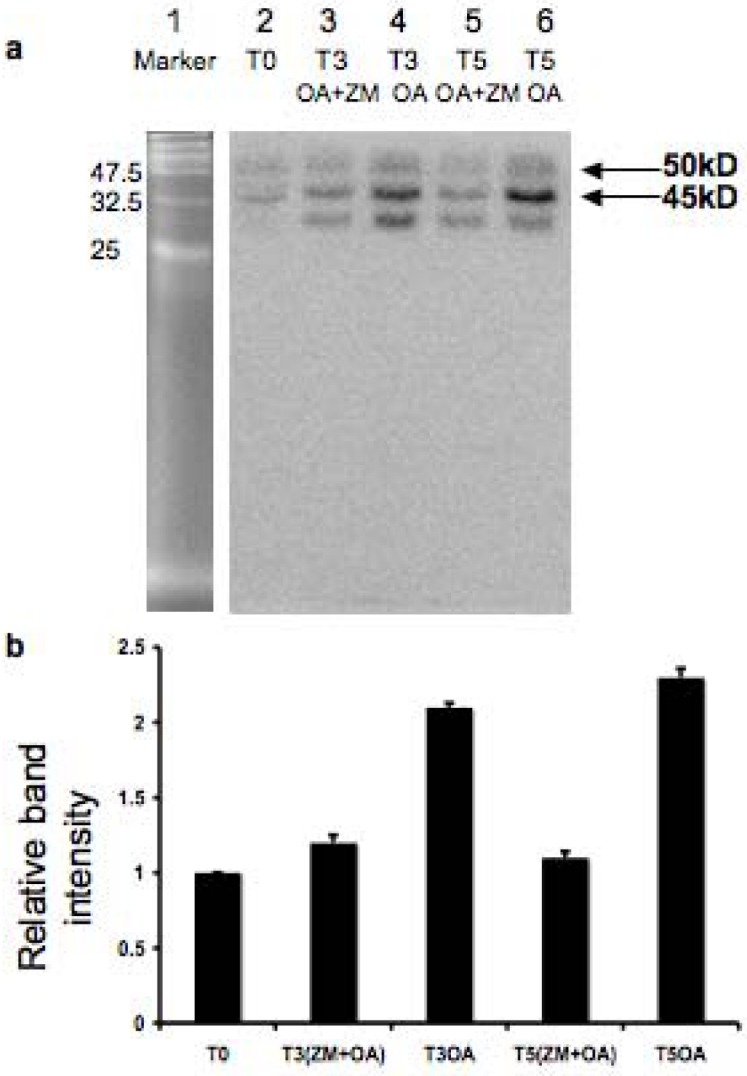

Figure 6.

OA activation and ZM inhibition of AURKs, as shown by an in-gel assay of aurora kinase activity. OA and ZM were used at the concentration of 5 μM and 5 μM, respectively, and cells were collected at 0 (T0), 3.0(T3), and 5.0 (T5) hours after incubation with or without treatment. Panel **a** is a representative gel, showing that OA -induced activation of AURKs is inhibited by ZM. The marker proteins were run on the same gel, and photographed before radioisotopic detection of kinase activity. The kinase activity migrating at 50 and 45 KDa is the appropriate size for active AURKA and AURKB, respectively (Crosio et al. 2002); the band below does not correspond to a known size for AURKs. Panel **b** shows the results of densitometric analysis of the 45 KDa AURKB band, where the activity of AURKs at T0 (time zero) was set as 1 for normalization of the other treatment groups This analysis was repeated three times. The data are presented as means ± SEM.

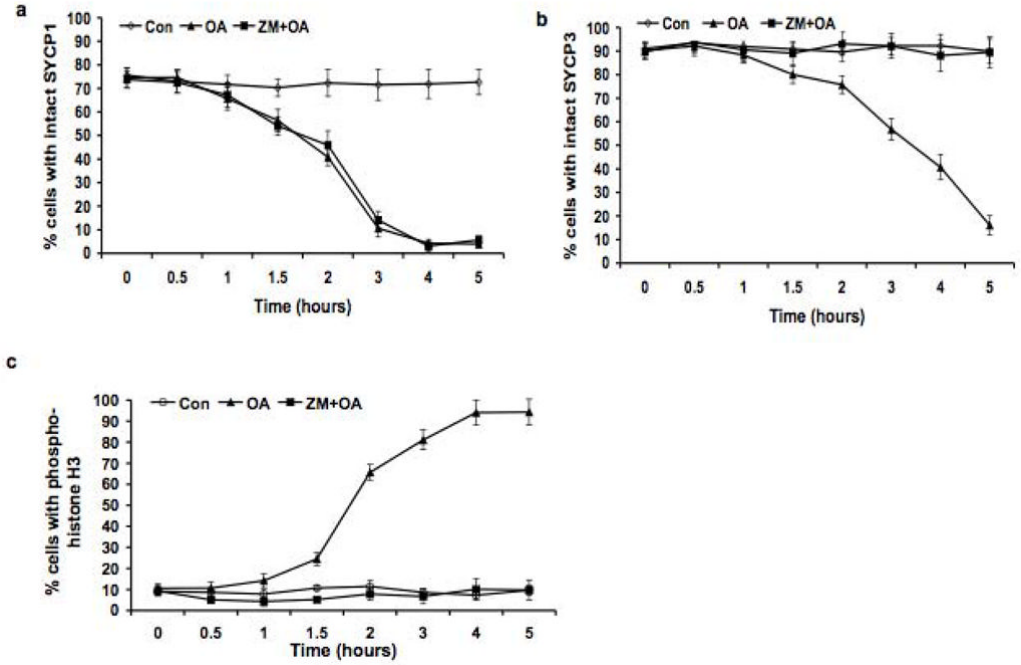

Figure 7.

ZM inhibition of SYCP3 removal from SC LEs and histone H3 phosphorylation on Ser10, but not of removal of SYCP1 (desynapsis). Panel **a** shows the dynamics of the removal of SYCP1 (desynapsis) in each experimental group. Panel **b** shows the removal of SYCP3 from the SC LEs in each experimental group. Panel c shows the increase in histone H3 phosphorylated on Ser10 in each experimental group. The frequency (%) of cells with uninterrupted (intact), pachytene-like signal for SYCP1 and SYCP3 was scored. 200 cells were scored for SYCP1 and SYCP3, and the experiment was repeated three times (a total of 600 cells scored); 200 cells were scored for histone H3 phosphorylated on Ser10, and the experiment was repeated three times (a total of 600 cells scored). ◇: Untreated control (Con) cells; ▲: cells treated with 5 μMOA (OA); ■: cells treated with 5 μMZM + 5 μMOA (ZM + OA). The data are presented as means ± SEM.

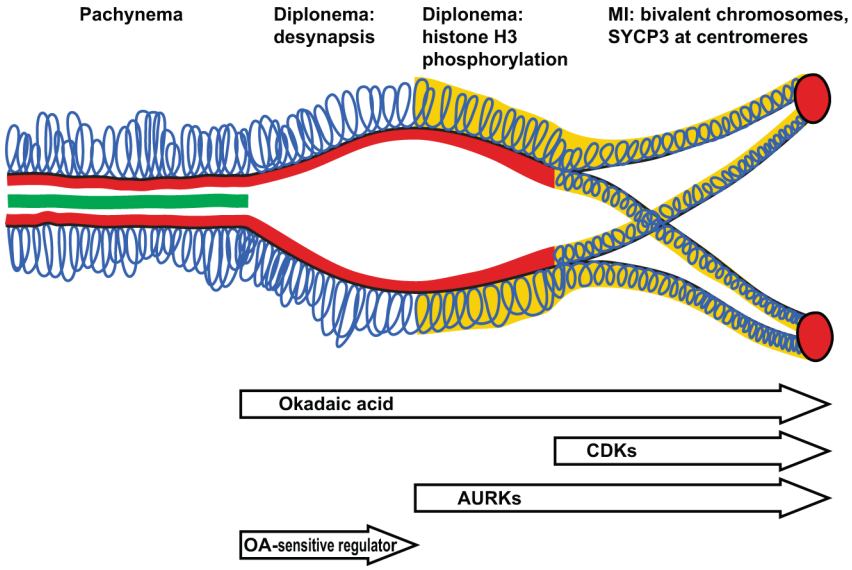

Figure 8.

A schematic representation of the G2/MI transition, reflecting the temporal course of events and differential inhibitor effects revealed in this study. At the pachytene stage, chromatin loops (blue) are attached to the SC LEs, marked by SYCP3 (red), and synapsis is mediated by SYCP1 (green) in the central element of the SC. OA (top arrow) prompts desynapsis and all subsequent events of the G2/MI transition. Desynapsis (removal of SYCP1 and disassembly of the SC central element) marks the onset of the diplotene stage. Histone H3 phosphorylated on Ser10 (yellow) accumulates in the chromatin during diplonema, but only after desynapsis occurs. Subsequently, the chromatin condenses further and SYCP3 is both removed and redistributed in the SC LEs to the centromeres and interchromatid patches, concurrent with condesation of bivalent chromosomes at MI. Inhibition of CDKs by BLI reveals that CDKs affect relocalization of SYCP3 and chromosome condensation. Inhibition of AURKs by ZM reveals that AURKs control phosphorylation of histone H3 on Ser10 in meiosis, as well as affecting subsequent events of SYCP3 relocalization and final condensation of bivalents. Neither BLI nor ZM affects OA-induced desynapsis; thus this event is controlled by an as-yet unidentified OA-sensitive regulator.